One Stroke Complementarity for Poisson-Like Problems

Ruben Specogna

Dipartimento di Ingegneria Elettrica, Gestionale e Meccanica, Università di Udine, Udine 33100, Italy

Taking electrokinetics as a paradigm problem for the sake of simplicity, complementarity originates when an irrotational electric field and a solenoidal current density satisfying boundary conditions are in hand. We first compare three formulations to obtain a solenoidal current density, both in terms of pure computational advantage and in the ability to pursue symmetric energy bounds with respect to the standard electric scalar potential formulation. For these formulations, we devise post-processing techniques that promise to provide bilateral bounds in one stroke, hence requiring the solution of just one linear system.

Index Terms— **Complementarity, complementary-dual, error bounds, mixed-hybrid formulation, Poisson problem.**

I. Introduction

COMPLEMENTARITY [1], [2] exhibits the unique feature of providing rigorous tolerance intervals for lumped parameters as capacitance, resistance, inductance, or force along with the estimation of their values. It defines also a robust error estimator for an automatic mesh adaptivity—the so-called constitutive error [2]—that enables us to stop the simulation once the obtained error is below the user-defined tolerance. By considering the electrokinetic problem, complementarity requires us to compute an irrotational electric field together with a solenoidal current density. This contribution investigates various alternatives to obtain these fields.

Typically, an irrotational electric field and a solenoidal current density are found by solving a pair of boundary value problems (BVPs) [1]–[4]. The irrotational electric field is easily and efficiently obtained by the standard nodal finite-element (FE) formulation—referred to as $\mathcal{V}$ in this paper—based on the electric scalar potential $\mathbf{V}$ sampled on the nodes of the cell complex $\mathcal{K}$ represented by the usual $\mathbf{G}$, $\mathbf{C}$, and $\mathbf{D}$ incidence matrices [5]. It is not clear, however, what is the cheapest method to obtain a solenoidal current density. Section II analyzes four methods to obtain such a current density, in particular, a mixed-hybrid geometric formulation and one with unknown electric scalar potential on dual nodes of the dual complex $\tilde{\mathcal{K}}$ represented by the $\tilde{\mathbf{G}} = \mathbf{D}^T$, $\tilde{\mathbf{C}} = \mathbf{C}$, and $\tilde{\mathbf{D}} = -\mathbf{G}^T$ incidence matrices [5]. Section III elaborates the idea to achieve complementarity by solving just one linear system, with obvious advantages concerning the simulation speed. From the solution of one linear system, in fact, one may reconstruct also the solution of the complementary problem by clever manipulations and interpolations inspired by vertex reconstruction techniques used—for a different purpose—in many finite volumes schemes. Section IV shows the numerical results. The conclusions are drawn in Section V.

II. Geometric Complementary and Complementary-Dual Formulations

A solenoidal current density is usually obtained by the complementary formulation $\mathcal{T}$ based on the electric vector potential $\mathbf{T}$ [3], [4]. We note that the association of physical variables and role of physical laws are interchanged with respect to the $\mathcal{V}$ formulation. Namely, the current continuity law holds because of the vector potential, whereas Faraday's law is enforced with a linear system.

In complementary-dual formulations, only the association of the physical variables with geometric elements is interchanged with respect to the scalar potential $\mathcal{V}$ formulation, whereas the role of the two physical laws remain the same. That is, the scalar potential $\tilde{\mathbf{V}}$ in the dual nodes is defined through

$$\tilde{\mathbf{U}} = -\tilde{\mathbf{G}}\tilde{\mathbf{V}} + \tilde{\mathbf{U}}_s = -\mathbf{D}^T\tilde{\mathbf{V}} + \tilde{\mathbf{U}}_s \tag{1}$$

where $\tilde{\mathbf{U}}$ stores the electromotive forces (EMFs) on dual edges and $\tilde{\mathbf{U}}_s$ is used to enforce Dirichlet boundary conditions (BCS) [6]. In particular, we assume that the EMFs $\{U_i^{\mathcal{E}}\}_{i=1}^{N_e}$ with respect to a reference electrode $\mathcal{E}_0$ of the $\{\mathcal{E}_i\}_{i=1}^{N_e}$ electrodes placed on $\partial\mathcal{K}$ are assigned. A homogeneous Neumann BCS is enforced on $\partial\mathcal{K} \setminus \cup_{i=1}^{N_e}\mathcal{E}_i$. The discrete Faraday law $\mathbf{C}^T\tilde{\mathbf{U}} = \mathbf{0}$ is implicitly satisfied, since $\mathbf{C}^T\mathbf{D}^T = (\mathbf{DC})^T = \mathbf{0}$ holds [5], if $\mathbf{C}^T\tilde{\mathbf{U}}_s = \mathbf{0}$. In this paper, we propose a practical way to compute such $\tilde{\mathbf{U}}_s : \tilde{\mathbf{U}}_s = \sum_{i=1}^{N_e} U_i^{\mathcal{E}}\mathbf{e}^i$, where the entry of $\mathbf{e}^i$ relative to the dual edge $\tilde{e}$, dual to face f, is $\mathbf{D}(v, f)$ if $f \in \mathcal{E}_i$ and zero otherwise; v is the only element whose boundary contains f.

Then, we consider the resistance matrix $\mathbf{R}$, which relates currents on faces, stored in the array $\mathbf{I}$, to voltages $\tilde{\mathbf{U}}$ with

$$\tilde{\mathbf{U}} = \mathbf{RI} \tag{2}$$

where $\mathbf{R}$ is the approximate discrete counterpart of the Ohm's constitutive relation at continuous level and may be efficiently constructed—by simple closed form expressions avoiding any numerical quadrature—for any star-shaped polyhedral meshes as described in [7]. Finally, the current continuity law

$$\mathbf{DI} = \mathbf{0} \tag{3}$$

has to be enforced by the linear system of equations. In the following, we present two different complementary-dual formulations to obtain a solenoidal current $\mathbf{I}$.

A. Mixed-Hybrid Formulation

Similarly to mixed FEs (MFEs) [8], we first write a system with both $\mathbf{I}$ and $\tilde{\mathbf{V}}$ as unknowns

$$\mathbf{RI} + \mathbf{D}^T\tilde{\mathbf{V}} = \tilde{\mathbf{U}}_s \tag{4}$$

$$\mathbf{DI} = \mathbf{0}. \tag{5}$$

Manuscript received May 23, 2014; revised August 22, 2014; accepted September 11, 2014. Date of current version April 22, 2015. Corresponding author: R. Specogna (e-mail: ruben.specogna@uniud.it).

Color versions of one or more of the figures in this paper are available online at http://ieeexplore.ieee.org.

Digital Object Identifier 10.1109/TMAG.2014.2358264

Even though this saddle point problem may be casted as a symmetric and positive definite (SPD) system by the penalty method [8, p. 80], a smarter solution (formulation $\mathcal{H}$), inspired by mixed-hybrid FEs (MHFEs) [8], [6], involves a domain decomposition with as many sub-domains as mesh elements. That is, the number of faces is doubled and $\underline{\mathbf{I}}$ represents the current over doubled faces. Constitutive matrix $\underline{\mathbf{R}}$ becomes block diagonal, each block being the local resistance mass matrix of one element. Finally, incidence matrix $\underline{\mathbf{D}}$ contains the local incidence matrices of each element placed in the appropriate columns and $\underline{\tilde{\mathbf{U}}}_s$ is simply $\tilde{\mathbf{U}}_s$ mapped to the labels of the doubled faces. We first note that the dual edges are broken in two pieces and a scalar potential $\tilde{\mathbf{V}}^f$ associated to the barycenter of the faces is needed to impose the continuity of the scalar potential through elements. The current solenoidality is imposed in each element with $\underline{\mathbf{D}}\underline{\mathbf{I}} = \mathbf{0}$, (7). We have also to impose the continuity of the current between each pair of doubled faces with $\mathbf{N}\underline{\mathbf{I}} = \mathbf{0}$, (8). Matrix $\mathbf{N}$ has a number of faces as rows and a total number of doubled faces as columns. Its entries for the row f are the incidence numbers $\mathbf{D}(v_1, f)$ and $\mathbf{D}(v_2, f)$, where v_1 and v_2 are the two elements that share f. These two integers are placed in the appropriate columns corresponding to the labels of f in the doubled list of faces. Of course, for faces f lying in the boundary, there is only one such element, and matrix $\mathbf{N}$ is in this case used to enforce the current of the Neumann BCS. Dirichlet BCS are enforced by $\underline{\tilde{\mathbf{U}}}_s$ and by setting the entries of $\tilde{\mathbf{V}}^f$ to zero for additional dual nodes lying on the Dirichlet boundary. Finally, the constitutive relation (4) is now written in the half dual edges as (6). The mixed system (4) and (5) becomes[1] [8]

$$\underline{\mathbf{R}}\underline{\mathbf{I}} + \underline{\mathbf{D}}^T\tilde{\mathbf{V}} + \mathbf{N}^T\tilde{\mathbf{V}}^f = \underline{\tilde{\mathbf{U}}}_s \tag{6}$$

$$\underline{\mathbf{D}}\underline{\mathbf{I}} = \mathbf{0} \tag{7}$$

$$\mathbf{N}\underline{\mathbf{I}} = \mathbf{0}. \tag{8}$$

Since $\underline{\mathbf{R}}$ is block diagonal, by inverting $\underline{\mathbf{R}}$, it is possible to easily eliminate the currents unknowns as

$$\underline{\mathbf{D}}\underline{\mathbf{R}}^{-1}\underline{\mathbf{D}}^T\tilde{\mathbf{V}} + \underline{\mathbf{D}}\underline{\mathbf{R}}^{-1}\mathbf{N}^T\tilde{\mathbf{V}}^f = \underline{\mathbf{D}}\underline{\mathbf{R}}^{-1}\underline{\tilde{\mathbf{U}}}_s \tag{9}$$

$$\mathbf{N}\underline{\mathbf{R}}^{-1}\underline{\mathbf{D}}^T\tilde{\mathbf{V}} + \mathbf{N}\underline{\mathbf{R}}^{-1}\mathbf{N}^T\tilde{\mathbf{V}}^f = \mathbf{N}\underline{\mathbf{R}}^{-1}\underline{\tilde{\mathbf{U}}}_s. \tag{10}$$

Matrix $\mathbf{Q} = \underline{\mathbf{D}}\underline{\mathbf{R}}^{-1}\underline{\mathbf{D}}^T$ is diagonal, the scalar value $\mathbf{Q}(v, v)$ being easily computed locally in each element v by $\mathbf{D}_v(\mathbf{R}_v)^{-1}\mathbf{D}_v^T$, where $\mathbf{R}_v$ and $\mathbf{D}_v$ are the local resistance mass matrix and local volume-face incidence matrix, respectively. Since $\mathbf{Q}$ can be easily inverted, we can also eliminate the potential unknowns to obtain the SPD system

$$\mathbf{N}\mathbf{H}\mathbf{N}^T\tilde{\mathbf{V}}^f = \mathbf{N}\mathbf{H}\underline{\tilde{\mathbf{U}}}_s \tag{11}$$

where $\mathbf{H} = \underline{\mathbf{R}}^{-1} - \underline{\mathbf{R}}^{-1}\underline{\mathbf{D}}^T\mathbf{Q}^{-1}\underline{\mathbf{D}}\underline{\mathbf{R}}^{-1}$. The assembling of (11) is easily performed locally for each element such that both $\mathbf{N}$ and labeling of the doubled faces are not explicitly constructed. In fact, for element v, one first finds the $\mathbf{Q}(v, v) = \mathbf{D}_v(\mathbf{R}_v)^{-1}\mathbf{D}_v^T$ real number, then forms the local (4×4 for a tetrahedron) matrix $\mathbf{H}_v = \mathbf{R}_v^{-1} - \mathbf{R}_v^{-1}\mathbf{D}_v^T\mathbf{Q}^{-1}\mathbf{D}_v\mathbf{R}_v^{-1}$. Each element $\mathbf{H}_v(i, j)$ has to be assembled in the row corresponding to face i and column corresponding to face j by multiplying it by $\mathbf{D}(v, i)\mathbf{D}(v, j)$ to take into account the left and right multiplication by $\mathbf{N}$ and $\mathbf{N}^T$, respectively.

[1] In MHFE formulations unknowns are associated to elements and represent the average of the scalar potential in the cells. Moreover, Lagrange multipliers are usually employed in place of $\tilde{\mathbf{V}}^f$.

B. Formulation Based on Dual Discrete Hodge Operators

By substituting (2) and (1) in (3), an algebraic system with one unknown per element is obtained

$$\mathbf{D}\mathbf{R}^{-1}\mathbf{D}^T\tilde{\mathbf{V}} = \mathbf{D}\mathbf{R}^{-1}\tilde{\mathbf{U}}_s. \tag{12}$$

This approach, for general polyhedral meshes, is not feasible since the $\mathbf{R}^{-1}$ matrix is full. For tetrahedral meshes, a general technique to produce a dual discrete Hodge operator in the form of a sparse matrix has been presented in [9]. While it represents a great asset for explicit Yee-like schemes, it shows its limitations when applied to BVPs (formulation $\tilde{\mathcal{V}}$) due to the large matrix fill-in. A sparse SPD system is obtained by enforcing in (3) the zero current on faces with a homogeneous Neumann BCS.

Similar formulations that do not guarantee first-order convergence on vector fields as [10] are not considered.

III. One Stroke Complementarity

The key idea of this section is that the irrotational electric field and solenoidal current density do not necessarily have to be the solutions of BVPs. One may even use random fields for deriving the complementary bounds provided that they satisfy BCS. Nonetheless, we would like the bounds to be, if not the best possible ones—i.e., the ones of minimum energy and coenergy provided by solving two BVPs—at least ones that make the bilateral bounds converge to each other.

Bossavit [6] advocated the use of MHFE formulations to retrieve both energy bounds by solving just one linear system. Unfortunately, we are not aware of any benchmark, which shows how these bounds perform in practical problems. One of the aims of this paper is to perform such a benchmark and also show that one stroke complementarity [6] is not a peculiarity of mixed-hybrid formulations but holds for any other complementary or complementary-dual formulation. To this aim, we first introduce a fast post-processing technique that produces consistent $\tilde{\mathbf{V}}$ and $\tilde{\mathbf{V}}^f$ from the solution of the $\mathcal{T}$ formulation. Obviously, all other formulations do not require this step as they have the scalar potential on dual nodes readily available. Then, second-order accurate techniques to interpolate the scalar potential from dual nodes to the nodes of the mesh are compared to obtain a curl-free electric field together with the original solenoidal current density.[2]

A. Scalar Potential on Dual Nodes

Find $\tilde{\mathbf{U}} = \mathbf{R}\mathbf{I}$ from the solution of the $\mathcal{T}$ formulation. Then, run the following linear worst case complexity algorithm.

[2] A solenoidal current density may be obtained from the solution of the $\mathcal{V}$ formulation by projecting the current obtained by interpolation to the space of solenoidal currents. Yet, one stroke complementarity seems lost since the projection entails again the solution of a second linear system.

1) $\tilde{\mathbf{V}}^f = \mathbf{0}$ and $\tilde{\mathbf{V}} = \mathbf{0}$. Take a random additional dual node $\tilde{n} \in \mathcal{E}_0$ and set $\tilde{\mathbf{V}}^f_{\tilde{n}} = 0$. Put $\tilde{n}$ into a stack S.
2) While the stack S is nonempty do
   a) Remove $\tilde{n}$ from the top of the stack.
   b) For each dual edge $\tilde{e}$ such that $\tilde{n} \in \partial\tilde{e}$ do
      i) If the other dual node $\tilde{p}$ in $\partial\tilde{e}$ does not have the value already defined, compute it with $\tilde{\mathbf{V}}_{\tilde{p}} = \tilde{\mathbf{V}}_{\tilde{n}} + \tilde{\mathbf{G}}(\tilde{e}, \tilde{p})\tilde{\mathbf{U}}_{\tilde{e}}$. If $\tilde{n}$ and/or $\tilde{p}$ are additional dual nodes on the boundary, use $\tilde{\mathbf{V}}^f_{\tilde{n}}$ and/or $\tilde{\mathbf{V}}^f_{\tilde{p}}$ in place of $\tilde{\mathbf{V}}_{\tilde{n}}$ and $\tilde{\mathbf{V}}_{\tilde{p}}$. Put $\tilde{p}$ into S.

B. Vertex Reconstruction Techniques

The electric potential $\mathbf{V}_n$ on a node n placed on a Dirichlet boundary is set to the corresponding BCS value. Otherwise, $\mathbf{V}_n$ on node n (coordinates x_n, y_n, z_n) is obtained as a weighted average of potentials $\tilde{\mathbf{V}}$ on dual nodes that are dual to cells surrounding n.[3] Moreover, if n is on a Neumann boundary, also of the potentials $\tilde{\mathbf{V}}^f$ on additional dual nodes dual to faces incident to n that are subject to Neumann, BCS are used in the weighted average. Let us call all these N potentials involved in the reconstruction $\{\tilde{\mathbf{V}}^r_i\}_{i=1}^N$ and coordinates where they are sampled $\{x_i, y_i, z_i\}_{i=1}^N$. Therefore

$$\mathbf{V}_n = \frac{\sum_{i=1}^{N} w_i \tilde{\mathbf{V}}^r_i}{\sum_{i=1}^{N} w_i} \tag{13}$$

where w_i are suitable weights. In the following, we drop the sum indices for conciseness. The popular inverse distance averaging procedure, which is only first-order accurate, uses $w_i = 1/r_i$, where $r_i = (\delta x_i^2 + \delta y_i^2 + \delta z_i^2)^{1/2}$ and $\delta k_i = k_i - k_n, k \in \{x, y, z\}$. We consider the second-order accurate *pseudo-Laplacian averaging* [11] instead, that uses $\sum w_i\, \delta x_i = 0$, $\sum w_i\, \delta y_i = 0$, $\sum w_i\, \delta z_i = 0$ to guarantee the exactness over affine data. Using Lagrange multipliers $\mathbf{\Lambda} = [\lambda_x, \lambda_y, \lambda_z]^T$, a minimization problem—that tries to keep weights as close to unity as possible—has to be solved [11]

$$\begin{bmatrix} \sum \delta x_i^2 & \sum \delta x_i\, \delta y_i & \sum \delta x_i\, \delta z_i \\ \sum \delta x_i\, \delta y_i & \sum \delta y_i^2 & \sum \delta y_i\, \delta z_i \\ \sum \delta x_i\, \delta z_i & \sum \delta y_i\, \delta z_i & \sum \delta z_i^2 \end{bmatrix} \mathbf{\Lambda} = -\mathbf{b} \tag{14}$$

where $\mathbf{b} = [\sum \delta x_i, \sum \delta y_i, \sum \delta z_i]^T$. Weights are obtained as $w_i = 1 + \lambda_x\, \delta x_i + \lambda_y\, \delta y_i + \lambda_z\, \delta z_i$. Alternatively, one may use a second-order technique based on *linear least squares* [12]. By describing the potential inside the dual volume as an affine function $v(x, y, z) = a + b\,(x - x_n) + c\,(y - y_n) + d\,(z - z_n)$, least squares are used to find $\mathbf{w} = [a, b, c, d]^T$ that minimizes the quadratic function[4] $\sum(\tilde{\mathbf{V}}^r_i - v(x_i, y_i, z_i))^2$.

[3] If cells surrounding n are not made of the same material, we select the material m with the greatest number of associated cells and use only the subset of cells with material m in the reconstruction.

[4] One may also use *weighted least squares*, for example by assigning bigger weights to closer nodes, but the reconstruction is not improved sensibly.

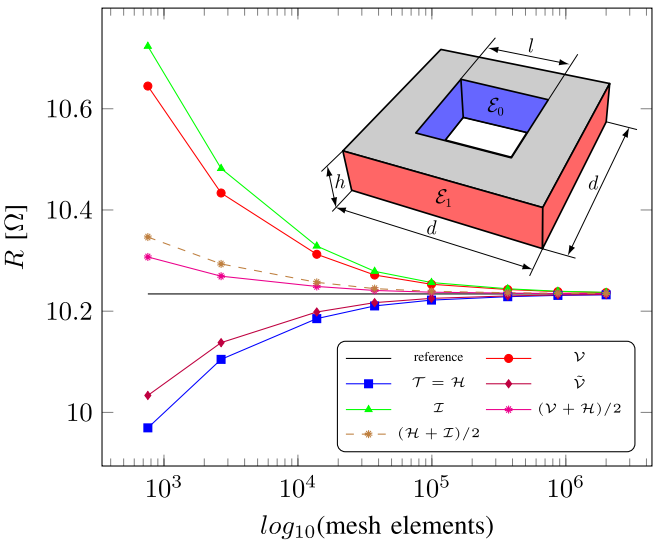

Fig. 1. Geometry of the square resistor and convergence of the resistance value with respect to an increasing number of mesh elements.

Thus, $\mathbf{V}_n = v(x_n, y_n, z_n) = \mathbf{w}(1) = a$ is found by solving the fundamental equations [12]

$$\mathbf{A}^T\mathbf{A}\mathbf{w} = \mathbf{A}^T\left[\tilde{\mathbf{V}}^r_1, \ldots, \tilde{\mathbf{V}}^r_N\right]^T \tag{15}$$

where the ith row of $\mathbf{A}$ is $[1, \delta x_i, \delta y_i, \delta z_i]$.

IV. Numerical Results

The algebraic multigrid code AGgregation-based algebraic MultiGrid [13] is used to solve the systems arising from $\mathcal{V}$, $\mathcal{H}$, and $\tilde{\mathcal{V}}$ formulations, whereas $\mathcal{T}$ formulation uses an in-house implemented conjugate orthogonal conjugate gradient with a hierarchically semiseparable preconditioner (relative residual is set to 1e-8 for both solvers.). All computations are run on an Intel Core i7-3720QM at 2.60 GHz laptop with 16 Gb of RAM.

All formulations fulfill the piecewise uniform current density patch test consisting of a planar resistor fed by electrodes placed at two parallel planes of a cube. The resistor is made of two materials of resistivity 1 and 100 Ωm such that the interface between them is parallel to the electrodes and divides the resistor in half. Moreover, the two second-order interpolation techniques are able to reconstruct the $\mathcal{V}$ solution from the $\mathcal{T}$, $\mathcal{H}$, or $\tilde{\mathcal{V}}$ solution up to machine precision.

In the following, $\mathcal{I}$ indicates that the results obtained with vertex reconstruction (pseudo-Laplacian averaging and least squares) give roughly the same results. We also remark that the solutions obtained by $\mathcal{T}$ and $\mathcal{H}$ formulations are always the same up to machine precision. The same holds for the potential on dual nodes reconstructed as described in Section III-A with respect to the one directly obtained by the $\mathcal{H}$ formulation.

A further code validation is performed by computing the resistance of a square resistor ($h = 1$ m, $d = 4$ m, and $l = 2$ m) (Fig. 1). Fig. 1 compares how the resistance computed by the various techniques converges to the exact solution (reference) when the number of elements is adaptively increased. Fig. 3(a) shows the time required for each formulation.

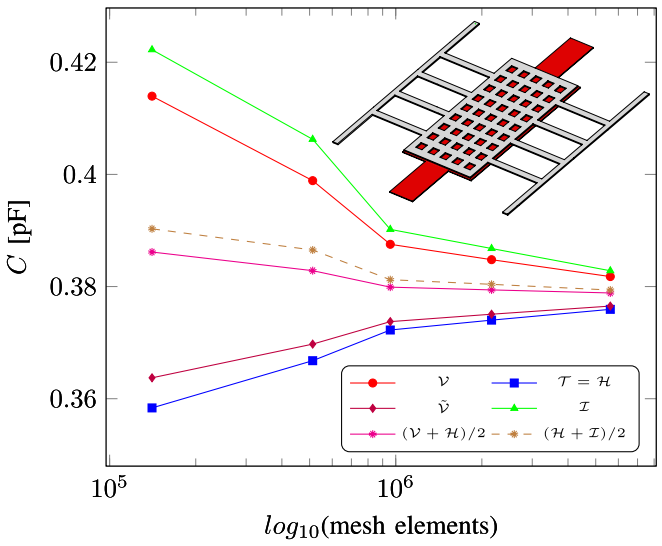

Fig. 2. Geometry of the capacitive MEMS switch and convergence of the capacitance value with adaptive mesh refinement.

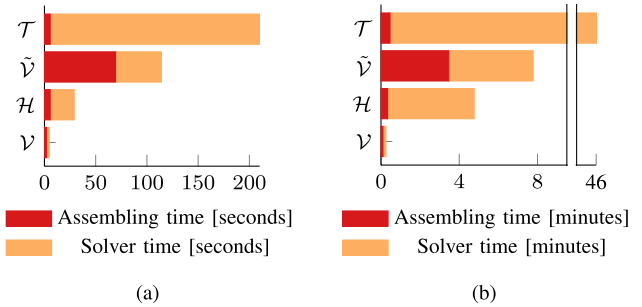

Fig. 3. (a) Simulation time for the square resistor on the finest mesh of about two million elements. (b) Simulation time for the MEMS problem on the finest mesh (∼5.6 million tetrahedra, 1.1 million nodes). The nonzero entries of the sparse matrix for the $\mathcal{V}$, $\mathcal{H}$, $\tilde{\mathcal{V}}$, and $\mathcal{T}$ formulations are 5.9, 43.2, 191.9, and 58.3 millions, respectively.

As a more complicated test case, the capacitive MEMS switch benchmark described in [4] and [14] is used (Fig. 2). In [14], the capacitance obtained with COMSOL (www.comsol.com) is 0.37 pF, with COVENTOR (www.coventor.com) 0.40 pF and GetDP (www.geuz.org/getdp) 0.36 pF. The results obtained with the techniques described in this paper are reported in Fig. 2. As Fig. 3(b) shows, the time required to solve the $\mathcal{H}$ system is roughly the same as the $\tilde{\mathcal{V}}$ one (typically, as in the previous example, $\mathcal{H}$ formulation is sensibly faster.) Nonetheless, the $\tilde{\mathcal{V}}$ formulation requires a considerable time during the assembling of $\mathbf{R}^{-1}$ matrix as described in [9]. This is because it needs to invert for each node a matrix whose dimension is the number of faces incident to that node (32 on average). This inversion is performed in parallel with `dgetrf` (LU factorization) and `dgetri` routines of the Intel MKL library.

V. Conclusion

Complementary error bounds are obtained for the first time in one stroke, i.e., using the solution of only one linear system. This reduces the required computational time to obtain the bounds since the cost of vertex reconstruction is negligible. While all complementary and complementary-dual formulations may benefit from one stroke complementarity, the mixed-hybrid formulation is typically faster on tetrahedral meshes. An even more efficient formulation, still valid only for isotropic materials, is described in [15]. The bilateral bounds on global parameters obtained by the mixed-hybrid formulation together with vertex reconstruction are fairly symmetric with respect to the exact solution, thus usually there is an accuracy improvement by considering the mean of the values obtained by the two methods. Either way, obtaining the bounds for free is interesting on its own.

Concerning the accuracy of the results in a given time, complementarity faces direct competition with the second-order FE formulation based on scalar potential, especially when high accuracy is required. For 2-D problems, an evaluation has been performed in [16]. A thorough comparison between these two approaches for 3-D problems is left for further studies. Nonetheless, we remark that, as far as we know, the second-order FE formulation is not able to produce bilateral energy bounds in one stroke, which is the theme of this paper.

References

[1] J. L. Synge, *The Hypercircle in Mathematical Physics*. New York, NY, USA: Cambridge Univ. Press, 1957.
[2] J. Rikabi, C. F. Bryant, and E. M. Freeman, "An error-based approach to complementary formulations of static field solutions," *Int. J. Numer. Methods Eng.*, vol. 26, no. 9, pp. 1963–1987, 1988.
[3] Z. Ren, "A 3D vector potential formulation using edge element for electrostatic field computation," *IEEE Trans. Magn.*, vol. 31, no. 3, pp. 1520–1523, May 1995.
[4] R. Specogna, "Complementary geometric formulations for electrostatics," *Int. J. Numer. Methods Eng.*, vol. 86, no. 8, pp. 1041–1068, 2011.
[5] E. Tonti, *The Mathematical Structure of Classical and Relativistic Physics*. Basel, Switzerland: Birkhäuser, 2013.
[6] A. Bossavit, "Mixed-hybrid methods in magnetostatics: Complementarity in one stroke," *IEEE Trans. Magn.*, vol. 39, no. 3, pp. 1099–1102, May 2003.
[7] L. Codecasa, R. Specogna, and F. Trevisan, "A new set of basis functions for the discrete geometric approach," *J. Comput. Phys.*, vol. 229, no. 19, pp. 401–410, 2010.
[8] F. Brezzi and M. Fortin, *Mixed and Hybrid Finite Element Methods*. New York, NY, USA: Springer-Verlag, 1991.
[9] L. Codecasa, R. Specogna, and F. Trevisan, "The discrete geometric approach for wave propagation problems," in *Proc. Int. Conf. Electromagn. Adv. Appl. (ICEAA)*, Turin, Italy, Sep. 2009 pp. 59–62.
[10] Z. Ren and X. Xu, "Dual discrete geometric methods in terms of scalar potential on unstructured mesh in electrostatics," *IEEE Trans. Magn.*, vol. 50, no. 2, Feb. 2014, Art. ID 7000704.
[11] D. G. Holmes and S. D. Connell, "Solution of the 2D Navier–Stokes equations on unstructured adaptive grids," in *Proc. 9th CFD Conf.*, 1989, doi:10.2514/6.
[12] G. Strang, *Introduction to Linear Algebra*. Cambridge, MA, USA: Wellesley-Cambridge, 2009.
[13] Y. Notay, "Aggregation-based algebraic multigrid for convection-diffusion equations," *SIAM J. Sci. Comput.*, vol. 34, no. 4, pp. A2288–A2316, 2012.
[14] R. V. Sabariego, J. Gyselinck, P. Dular, J. De Coster, F. Henrotte, and K. Hameyer, "Coupled mechanical-electrostatic FE-BE analysis with FMM acceleration: Application to a shunt capacitive MEMS switch," *COMPEL Int. J. Comput. Math. Elect. Electron. Eng.*, vol. 23, no. 4, pp. 876–884, 2004.
[15] R. Specogna, "Diagonal discrete Hodge operators for simplicial meshes using the signed dual complex," in *Proc. IEEE CEFC*, 2014, doi: 10.1109/TMAG.2014.2350515.
[16] R. Specogna, "Extraction of VLSI multiconductor transmission line parameters by complementarity," *IEEE Trans. Very Large Scale Integr. (VLSI) Syst.*, vol. 22, no. 1, pp. 146–154, Jan. 2014.